frontiers | Frontiers in Marine Science

ORIGINAL RESEARCH
published: 10 June 2022
doi: 10.3389/fmars.2022.920745

Trophic Diversity and Food Web Structure of Vegetated Habitats Along a Coastal Topographic Gradient

Xiaoxiao Li[1,2], Wei Yang[3,4], Tao Sun[3,4] and Zhifeng Yang[1,2*]*

[1] Guangdong Provincial Key Laboratory of Water Quality Improvement and Ecological Restoration for Watersheds, School of Ecology, Environment and Resources, Guangdong University of Technology, Guangzhou, China, [2] Southern Marine Science and Engineering Guangdong Laboratory (Guangzhou), Guangzhou, China, [3] State Key Laboratory of Water Environment Simulation, School of Environment, Beijing Normal University, Beijing, China, [4] Yellow River Estuary Wetland Ecosystem Observation and Research Station, Ministry of Education, Shandong, China

OPEN ACCESS

Edited by:
Tian Xie,
Beijing Normal University, China

Reviewed by:
Lei Zhao,
China Agricultural University, China
Jianfeng Feng,
Nankai University, China

***Correspondence:**
Wei Yang
yangwei@bnu.edu.cn
Zhifeng Yang
zfyang@gdut.edu.cn

Specialty section:
This article was submitted to
Marine Ecosystem Ecology,
a section of the journal
Frontiers in Marine Science

Received: 15 April 2022
Accepted: 16 May 2022
Published: 10 June 2022

Citation:
Li X, Yang W, Sun T and Yang Z (2022)
Trophic Diversity and Food Web
Structure of Vegetated Habitats Along
a Coastal Topographic Gradient.
Front. Mar. Sci. 9:920745.
doi: 10.3389/fmars.2022.920745

Land–sea interactions in coastal wetlands create heterogeneous vegetated habitats with regular zonation along a topographic gradient. However, it's unclear how the trophic diversity of communities and trophic structure of food webs change along the gradient. Here, we investigated the empirically resolved food web structure and trophic diversity across four vegetated habitats (*Phragmites australis*, *Suaeda salsa*, *Spartina alterniflora*, and *Zostera japonica* seagrass) along a gradient from upland to near-shore waters in the Yellow River Delta wetland. We quantified $\delta^{13}C$ and $\delta^{15}N$ of carbon sources (detritus, primary producers) and consumers (zooplankton, macroinvertebrates, fish). $\delta^{13}C$ and $\delta^{15}N$ of the carbon sources and consumers differed significantly among the four habitats. Carbon sources and consumers became more ^{13}C-enriched and ^{15}N-enriched along the gradient, respectively. The consumer trophic position was higher in the *S. salsa* habitat than in the seagrass habitat, followed by the *S. alterniflora* and *P. australis* habitats. The habitat formed by invasive *S. alterniflora* had the lowest corrected standard ellipse areas in the $\delta^{13}C$ vs. $\delta^{15}N$ plots for the basal carbon sources and all consumers combined, and the lowest Layman community metrics for the $\delta^{13}C$ range, total area, and centroid distance; thus, trophic groups in this habitat had the lowest isotopic trophic diversity. Using a Bayesian isotope mixing model, we found that consumer diet compositions differed greatly among the habitats where the consumer was present, except for shrimps and polychaetes. Food web topological properties (species richness, number of trophic links, linkage density, proportions of intermediate consumers and omnivores) increased along the gradient. Generally, habitat heterogeneity created highly variable food webs. Our results provide insights into the spatial variation in coastal ecosystems along a topographic gradient, and demonstrate the need to protect habitat heterogeneity in coastal wetlands, combined with adaptive management to control invasive species.

Keywords: food web, trophic structure, trophic diversity, stable isotope, plant zonation, coastal wetland

INTRODUCTION

Coastal wetlands are located in the ecotone between land and sea, and exhibit strong natural habitat heterogeneity, with upland, salt marsh, mudflat, and near-shore waters. These habitats display significant topographic gradients for parameters such as salinity, elevation, and flooding frequency (Barbier et al., 2011; Rogers et al., 2019). The environmental variation along the gradient has significant structural effects on the spatial distributions and characteristics of biotic communities (Bang et al., 2018; Janousek et al., 2019; Colombano et al., 2021). In particular, they form a vegetation mosaic (a plant zonation pattern) along the gradient (Pennings et al., 2005; Cui et al., 2011; Engels et al., 2011). Given that different communities respond differently to their different trophic niches, stress tolerance, and life history (Li et al., 2020). This variation ultimately leads to different overall food web characteristics that result from complex trophic cascade interactions.

The vegetated habitats along a coastal topographic gradient also show large variations in carbon sources at the base of their food webs, including differences between C4 salt marsh plants (e.g., *Phragmites australis*, *Suaeda salsa*) and C3 plants (e.g., *Spartina alterniflora*, *Zostera japonica*) (Zhang et al., 2010; Christianen et al., 2017). The intermediate consumers were dominated by insects at upland sites, but shifted to bivalves and gastropods in the near-shore waters (Dauer et al., 2010; Li et al., 2020). Furthermore, the complexity of coastal food webs increases due to couplings between green and brown food chains (Nordström et al., 2015; Schrama et al., 2017), and between pelagic and benthic trophic pathways (Kopp et al., 2015; Jones et al., 2021). Most researchers have investigated food web characteristics for a specific coastal habitat, most commonly for salt marsh habitats (Marczak et al., 2011; Nordström et al., 2015; Schrama et al., 2017; Baker et al., 2021). However, one of the most pressing challenges is to empirically investigate the spatial variations of food webs along a large coastal topographic gradient that includes multiple habitats, thereby improving our understanding of coastal ecosystem structure and functioning (Tylianakis and Morris, 2017; Baiser et al., 2019).

Available studies have mainly addressed changes in the trophic structure of coastal food webs along latitudinal gradients (Saporiti et al., 2015; Cardona et al., 2021), or gradients in nutrient enrichment and hydraulic residence time (Sierszen et al., 2006). In addition, some studies examined changes in food web properties in diverse wetland habitats along a water-flow gradient from the upper river estuary to coastal offshore waters (Kim et al., 2020; Kundu et al., 2021). For example, Vinagre and Costa (2014) revealed that the upper estuary had higher variability for many topological properties, but did not differ significantly from that in the lower estuary.

Studies of the plant zonation patterns along coastal topographic gradients have compared food web characteristics between *P. australis* and *S. salsa* habitats (Park et al., 2015) and between *P. australis* and *S. alterniflora* habitats (Dibble and Meyerson, 2014). However, information is still lacking on generalized patterns in terms of the trophic structure and associated food web properties across more variable vegetated habitats along the topographic gradient, and this limits our understanding of how coastal gradients shape heterogeneous food webs in coastal wetlands.

The Yellow River Delta wetland has a complex coastal system and provides an ideal topographic gradient that can be used to assess changes in the food web trophic structure among variable vegetated habitats due to its distinct plant zonation patterns. The plant communities are dominated by *P. australis*, *Tamarix chinensis*, *S. salsa*, *S. alterniflora*, and *Z. japonica* seagrass (from upland to near-shore waters) in this coastal wetland (Cui et al., 2011; Qi et al., 2021). Using this area as our case study, we investigated the spatial variation of food webs across four different vegetated habitats along the topographic gradient from upland to the near-shore waters. Specifically, our objectives were: (1) to investigate changes in stable carbon and nitrogen isotope values in the trophic groups as well as variations in the trophic position of consumers along the gradient, (2) to investigate changes in isotopic niche characteristics of the trophic groups that represent their trophic diversity along the gradient, and (3) to investigate changes in the topological properties of food web networks, quantitative diet compositions of consumers, and food web trophic structure along the gradient. We hypothesized that the food web characteristics would vary significantly along the gradient, reflecting differences in ecosystem functioning among the vegetated habitats. In addition, based on previous measurements of species composition and biomass distribution in the biotic communities along the topographic gradient in the Yellow River Delta (Li et al., 2020), we hypothesized that the food webs at low elevations in the coastal wetland would be more complex than those at higher elevations in terms of the complexity of the topological properties.

MATERIALS AND METHODS

Study Area

Our study was conducted in a coastal wetland within China's Yellow River Delta national nature reserve, where the Yellow River enters the Bohai Sea on the Pacific coast of northeastern China (**Figure 1**). This delta is the largest, youngest, most active, and most fragile estuary wetland in China. It has a warm temperate continental monsoon climate with distinct seasons and irregularly semidiurnal (twice daily) tides. The average annual temperature is 12°C, with mean monthly temperatures ranging from -3°C in January to 27°C in July, and the average annual precipitation and evaporation are 552 mm and 1962 mm, respectively (Cui et al., 2011).

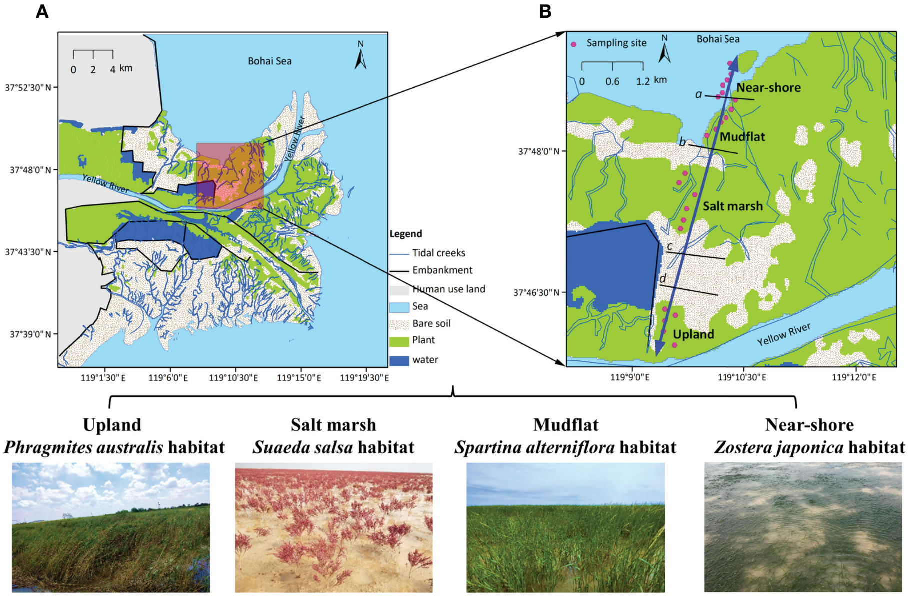

FIGURE 1 | **(A)** Map of China's Yellow River Delta based on the interpretation of remote sensing images from 2015. **(B)** Location of the four studied vegetated habitats along a topographic gradient: *Phragmites australis* habitat in the upland, *Suaeda salsa* habitat in the salt marsh, *Spartina alterniflora* in the mudflat, and *Zostera japonica* seagrass habitat in the near-shore waters. The black lines represent the approximate borders between adjacent habitats; thus, the lines marked with *c* and *d* represent the borders between the marsh and the terrestrial border and between the terrestrial border and the upland habitat, which developed at the highest astronomical tide based on data from Cui et al. (2011) and Li et al. (2020). Photos were taken by X. Li in 2019.

Fieldwork was conducted on the northern shore of the Yellow River channel. There is no tidal embankment along the coastline. Due to the interactions between land and sea, environmental factors vary greatly along the topographic gradient, with the elevation ranging from 0 m at the seashore to 2.5 m at the upland sites; as a result, the flooding frequency ranges from 0% at the upland sites to 95% at the seashore (Cui et al., 2011). The water salinity ranges from <0.5‰ at the upland sites to 30‰ at the seashore (Li et al., 2020). Clear plant zonation patterns are visible along the gradient (Qi et al., 2021). We selected four habitats with different vegetation communities for our study: the *P. australis* upland, the *S. salsa* salt marsh, the habitat of invasive *S. alterniflora* in the mudflat area, and the *Z. japonica* seagrass habitat in the near-shore waters (**Figure 1**). In each habitat, we performed sampling at 6 sites (**Figure 1B**). The macroinvertebrate community also showed large variation across the four habitats, and the dominant macroinvertebrate species changed from insects in the upland habitat to bivalves and gastropods closer to the sea (Li et al., 2020). The large variations in abiotic and biotic factors among the four habitats enable us to further explore the spatial variations in food web characteristics, thereby enriching our understanding of the spatial variation in food web dynamics along the coastal gradient.

Sample Collection and Processing

To determine the spatial variations in food web characteristics across the four vegetated habitats along the coastal topographic gradient, we collected samples of food web items from each habitat in September 2018 and June, July, and August 2019, to cover most of the growing season. We collected potential carbon sources at the base of the food webs, consisting of sediment organic matter (SOM), particulate organic matter (POM), C3 and C4 vascular plants, microphytobenthos, and phytoplankton. We collected zooplankton, macroinvertebrates, and fish to represent consumers in these food webs.

Bulk sediment was collected using a soil core sampler (5.0 cm in diameter, 5.0 cm in depth) to prepare samples of SOM. Water samples were collected at a depth of 20 cm in tidal creeks using a Plexiglass water collector. We filtered the water column through a 200-μm mesh to remove large detritus and then acquired samples of POM by rinsing the samples on pre-combusted (450° C for 6 h) glass-fiber filters (0.45 μm, Whatman GF/F; Mao et al., 2016). We collected fresh leaves of vascular plants by hand and washed them with distilled water. Microphytobenthos samples were collected by scraping the surface of stones in the tidal creek (O'Gorman et al., 2017). Phytoplankton and zooplankton samples were collected by filtration of the collected water column through meshes with sizes of 0.064 and 0.122 mm, respectively. They were then rinsed onto pre-combusted glass-fiber filters for stable isotope determination. Macroinvertebrates were collected by dredging the sediment to a depth of 20 cm. The sediment was then washed and passed through a 0.5-mm mesh to extract organisms. Fish were collected by employing fishing cages in tidal creeks (sampling details see Li et al., 2020).

Different pre-treatments were applied to these organisms before determining the stable isotopic values for carbon ($\delta^{13}C$) and nitrogen ($\delta^{15}N$). For shrimp, we removed the entire shell, head, and tail, and then extracted the muscle tissue. For crabs, we extracted muscle tissue from the large claw. For snails and bivalves, we removed the viscera from the shell. We used the entire body for other small organisms. For fish, we extracted the white dorsal muscle tissues from three individuals per species with similar size or weight to provide a single composite sample for isotope detection. All stable isotope samples were oven-dried at 60°C to constant weight, then ground into a fine powder using a mortar and pestle. Stable isotope analysis was performed in a continuous-flow isotope-ratio mass spectrometer (Delta V Advantage, Thermo Scientific, Schwerte, Germany) coupled with an elemental analyzer (Flash EA1112, Thermo Scientific, Monza, Italy). We recalibrated the spectrometer after every 10 measurements. Measurement precision of $\delta^{13}C$ and $\delta^{15}N$ were 0.1‰ and 0.2‰, respectively. We used Vienna PeeDee Belemnite (VPDB) and atmospheric N_2, respectively, as the standard samples to calculate the $\delta^{13}C$ and $\delta^{15}N$ ratios. Since $\delta^{15}N$ ratios change as a result of trophic fractionation, we defined the trophic position (*TP*) of a consumer trophic group as follows (vander Zanden et al., 1999):

$$TP = \left[(\delta^{15}N_{\text{consumer}} - \delta^{15}N_{\text{baseline}}) / TEF\right] + 2 \qquad (1)$$

where $\delta^{15}N_{\text{consumer}}$ is the consumer's $\delta^{15}N$ value, and $\delta^{15}N_{\text{baseline}}$ is the baseline $\delta^{15}N$ value, which we assumed equaled the average value for all primary consumers (i.e., detritivores and herbivores) in each habitat. We assumed that the trophic enrichment factors (*TEF*) were 3.4 ± 1.0‰ (mean ± SD) for $\delta^{15}N$ and 0.4 ± 1.3‰ for $\delta^{13}C$, which are the values used in the SIAR model, according to Post (2002). The trophic position of the carbon sources was set to 1.

We divided the collected organisms into different trophic groups, which we defined as groups of taxa that share the same set of prey and predators (Dunne et al., 2002), for each habitat (**Supplementary Table 1**). In total, we collected 86 stable isotope samples for all trophic groups in the *P. australis* habitat (**Supplementary Table 2**), 113 samples in the *S. salsa* habitat (**Supplementary Table 3**), 131 samples in the *S. alterniflora* habitat (**Supplementary Table 4**), and 117 samples in the *Z. japonica* habitat (**Supplementary Table 5**).

Stable Isotope Data Analysis

The size of the region occupied by an assemblage in the stable isotope space (i.e., in the $\delta^{13}C$ vs. $\delta^{15}N$ plots) contains information about isotopically defined trophic diversity, and reflects the size of the trophic niche (Abrantes et al., 2014). Thus, the close proximity of consumer taxa in isotope space reflects potential trophic redundancy. To investigate differences in trophic niche size of all carbon sources, all consumers combined, and each consumer trophic group among the four habitats, we quantified the value of the corrected standard ellipse area (SEA_c, ‰^{2}) using the SIBER package (Stable Isotope Bayesian Ellipses in R, Jackson et al., 2011) implemented in R version 2.1.6 (https://www.r-project.org/). Higher values of SEA_c indicate wider isotopic trophic niches as well as higher trophic diversity of an assemblage of communities (Masese et al., 2018). For consumers, we further analyzed the percentage overlap of the 95% confidence interval for SEA_c between pairs of habitats. Values of this overlap range from 0% when the two ellipses are completely separated to 100% when they fully overlap. For a target consumer group, a high overlap between pairs of habitats implies that the consumer group relies on similar food sources within the two habitats, which means it has a similar trophic niche in both habitats; conversely, a low overlap means different food sources and trophic niches (Jackson et al., 2011).

We also analyzed the metrics proposed by Layman et al. (2007) to describe the trophic niche structure:

1. $\delta^{13}C$ range (*CR*), with a wide range representing niche diversification among carbon sources;
2. $\delta^{15}N$ range (*NR*), with a wide range suggesting trophic length;
3. total area (*TA*), which represents the area of the convex hull occupied by the assemblage in the $\delta^{13}C$ versus $\delta^{15}N$ isotopic space;
4. centroid distance (*CD*), which represents the Euclidean distance of each component of the species assemblage from the centroid;
5. mean nearest-neighbor distance (*MNND*), which represents the mean Euclidean distance from each group to its nearest neighbor in the isotopic space;
6. standard deviation of the nearest-neighbor distance (*SDNND*), which represents the evenness of the isotopic space for all species assemblages.

Lower values of *MNND* and *SDNND* indicate higher trophic redundancy; that is, a low *MNND* means more trophic groups with similar trophic ecologies, and a low *SDNND* means more evenly distributed species (Abrantes et al., 2014). To overcome the dependence of the six Layman metrics on sample size, we followed the advice of Jackson et al. (2011) and calculated the Bayesian *CR*, *NR*, *TA*, *CD*, *MNND*, and *SDNND* at each habitat using the SIBER package to provide unbiased and more robust metrics that accounted for variations in sample size in our statistical comparisons of the Layman metrics among the four studied habitats.

Bayesian Isotope Mixing Model

We derived the empirical food webs for the four vegetated habitats by combining literature analysis and the Bayesian isotope mixing model. We firstly derived the potential prey for each consumer trophic group in each habitat based on published diet data in similar coastal ecosystems or close to our study area (**see Supplementary diet literature**). Based on the information on potential food sources, we then ran the Bayesian stable isotope mixing model for each consumer to identify whether the potential feeding link described in the literature was valid at our study sites, and then obtained the quantitative contributions to each consumer's diet.

We created the Bayesian isotope mixing model using the SIAR package (Stable Isotope Analysis in R; Parnell et al., 2010) implemented in version 3.6.1 of the R software, which solves mixing models based on isotope data using a Markov-chain Monte Carlo approach, and simulates dietary proportions using a Dirichlet prior distribution (Parnell et al., 2010). We ran 30,000 iterations of each SIAR model, and the output represents a probability-density distribution for the potential contribution of each prey item to the diet of each consumer. We assigned a feeding link in the food web when the lower limit of the 50% credibility interval for the contribution of each source to the consumer's diet exceeded 5% (Careddu et al., 2015; Bentivoglio et al., 2016).

To characterize the trophic structure of food webs across the four habitats along the coastal gradient, we selected 12 commonly addressed topological properties:

1. richness (*S*), number of trophic groups in the food web;
2. links (*L*), number of trophic links between the trophic groups;
3. linkage density (*LD*), $LD = L/S$;
4. connectance (*C*), $C= L/S^2$;
5. top species (*T*), proportion of species that have no predators;
6. intermediate species (*I*), proportion of species that have both prey and predators;
7. basal species (*B*), proportion of species that have no prey;
8. omnivory (*O*), proportion of species that consume prey from more than one trophic level;
9. *GenSD*, standard deviation of the number of prey resources per species;
10. *VulSD*, standard deviation of the number of consumers for each species;
11. *ATL*, average trophic level;
12. *MaxSim*, maximum Jaccardian similarity.

We calculated these topological properties using the Network 3D software (Yoon et al., 2004; Williams, 2010).

Statistical Analysis

We used one-way ANOVA to identify significant differences in the $\delta^{13}C$ and $\delta^{15}N$ values of the trophic groups among the four habitats. When the ANOVA test showed a significant difference ($p < 0.05$), we used Tukey's HSD *post-hoc* test to identify significant differences between pairs of habitats. Statistical analyses were conducted using version 20.0 of the Statistical Package for the Social Sciences (SPSS) software (www.ibm.com/analytics/us/en/technology/spss/).

RESULTS

Signatures of Stable Isotope Values of Trophic Groups

$\delta^{13}C$ and $\delta^{15}N$ Values of Carbon Sources

The $\delta^{13}C$ values of the carbon sources (i.e., detritus and primary producers) differed significantly among sources in the *P. australis* habitat (**Supplementary Table 2**; one-way ANOVA, $F_{4,40} = 33.54$, $p < 0.001$), the *S. salsa* habitat (**Supplementary Table 3**; $F_{4,43} = 58.23$, $p < 0.001$), the *S. alterniflora* habitat (**Supplementary Table 4**; $F_{4,41} = 51.74$, $p < 0.001$), and the *Z. japonica* habitat (**Supplementary Table 5**; $F_{4,32} = 14.97$, $p < 0.001$). The highest range of mean $\delta^{13}C$ values of the carbon sources occurred in the *S. salsa* habitat (from -28.99 ± 0.63‰ to -5.46 ± 0.53‰, mean ± SD), followed by the *P. australis* habitat (from -25.74 ± 0.67‰ to -6.84 ± 0.75‰), the *Z. japonica* habitat (from -20.61 ± 3.60‰ to -5.62 ± 0.16‰) and the *S. alterniflora* habitat (from -19.90 ± 0.02‰ to -7.00 ± 0.79‰) (**Figure 2**).

In all four habitats, SOM was always the most ^{13}C-enriched carbon source (Tukey's HSD test, $p < 0.05$, **Supplementary Table 2 to 5**). In both the *P. australis* and *Z. japonica* habitats, phytoplankton (-20.28 ± 6.72‰ and -20.61 ± 3.60‰, respectively) was significantly more ^{13}C-depleted than microphytobenthos (-14.82 ± 1.37‰ and -12.97 ± 0.40‰, respectively). In the *S. salsa* habitat, *S. salsa* was the most ^{13}C-depleted basal source (-28.99 ± 0.63‰), with a value significantly lower than that of other carbon sources ($p < 0.05$; **Supplementary Table 3**). In the *S. alterniflora* habitat, phytoplankton (-13.65 ± 1.25‰) and *S. alterniflora* (-14.45 ± 1.45‰) were both significantly more ^{13}C-enriched than POM (-17.57 ± 2.24‰) and the microphytobenthos (-19.90 ± 0.02‰) (**Supplementary Table 4**).

The $\delta^{15}N$ values of the carbon sources also showed significant differences in the *S. salsa* habitat (ANOVA, $F_{4,43} = 6.37$, $p < 0.001$) and the *S. alterniflora* habitat ($F_{4,41} = 3.17$, $p = 0.02$), but there were no significant differences in the *P. australis* habitat ($F_{4,40} = 1.54$, $p = 0.21$) and the *Z. japonica* habitat ($F_{4,32} = 1.20$, $p = 0.33$). The $\delta^{15}N$ values of the carbon sources ranged from 1.61 ± 0.45‰ to 3.90 ± 2.84‰ in the *P. australis* habitat, from 4.05 ± 0.56‰ to 6.26 ± 0.78‰ in the *S. salsa* habitat, from 4.95 ± 0.46‰ to 6.65 ± 0.78‰ in the *S. alterniflora* habitat, and from 5.02 ± 1.20‰ to 6.68 ± 0.68‰ in the *Z. japonica* habitat. POM had significantly higher $\delta^{15}N$ values (6.26 ± 0.78‰) than phytoplankton (4.35 ± 1.97‰) in the *S. salsa* habitat ($p < 0.05$, **Supplementary Table 3**).

$\delta^{13}C$ and $\delta^{15}N$ Values of Consumers

Consumers also showed significant differences in $\delta^{13}C$ values among the four habitats (for the *P. australis* habitat, $F_{7,44} = 3.09$, $p = 0.01$; for the *S. salsa* habitat, $F_{9,68} = 3.41$, $p = 0.002$; for the *S. alterniflora* habitat, $F_{10,88} = 14.95$, $p < 0.001$; for the *Z. japonica* habitat, $F_{10,83} = 17.13$, $p < 0.001$). The distribution of the $\delta^{13}C$ values of consumers was relatively narrow in the *P. australis* habitat (from -25.06 ± 4.31‰ to -20.54 ± 3.83‰) compared to the ranges in the *S. salsa* habitat (from -20.01 ± 1.67‰ to -12.24 ± 2.01‰), the *S. alterniflora* habitat (from -22.44 ± 3.88‰ to -10.46 ± 4.19‰), and the *Z. japonica* habitat (from -27.01 ± 2.44‰ to -11.24 ± 2.67‰) (**Figure 2 and Supplementary Table 2 to 5**). Zooplankton showed more ^{13}C-depleted values in the *P. australis* (-22.61 ± 2.25‰) and *Z. japonica* (-23.70 ± 1.64‰) habitats than in the *S. salsa* (-14.99 ± 5.01‰) and *S. alterniflora* (-13.59 ± 1.21‰) habitats. The macroinvertebrate (mean for all groups ± SD, -22.73 ± 1.85‰) and fish (-23.25 ± 4.35‰) groups both had more ^{13}C-depleted values (in average) in the *P. australis* habitat than in the other habitats: for the *S. salsa* habitat, -16.20 ± 2.96‰ for macroinvertebrates and -17.66 ± 1.91‰ for fish; for the *S. alterniflora* habitat, -16.70 ± 3.68‰ for macroinvertebrates and -18.51 ± 3.03‰ for fish; for the *Z. japonica* habitat, -15.40 ± 3.23‰ for macroinvertebrates and -19.72 ± 3.30‰ for fish. This demonstrates that fish generally had more ^{13}C-depleted values than macroinvertebrates in the four habitats.

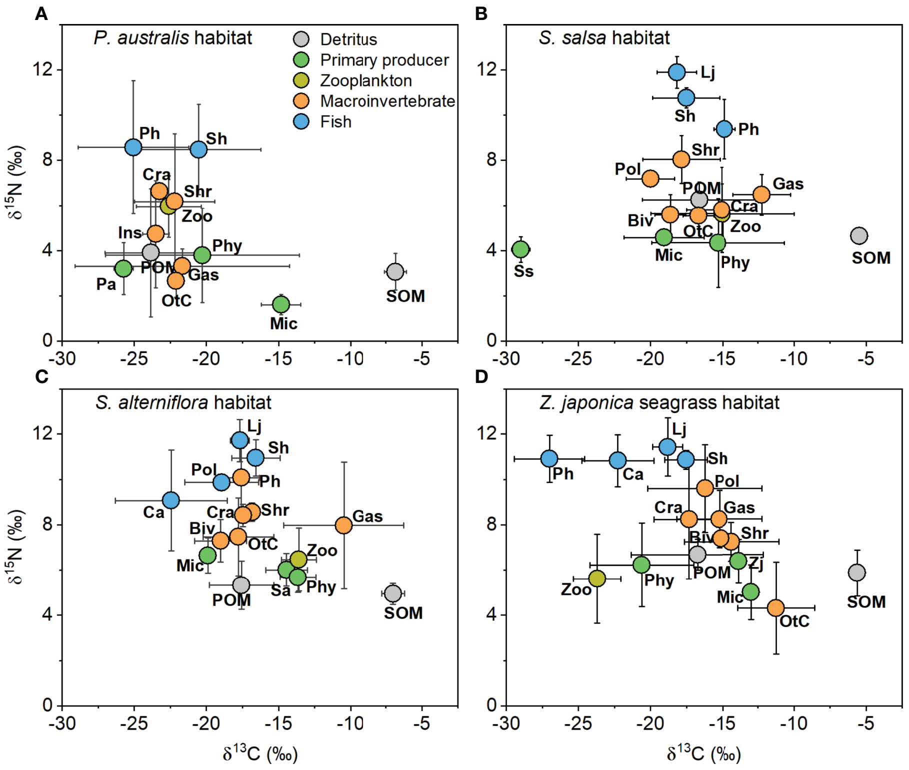

FIGURE 2 | δ^{13}C and δ^{15}N values (mean ± SD) of trophic groups collected from **(A)** *Phragmites australis*, **(B)** *Suaeda salsa*, **(C)** *Spartina alterniflora*, and **(D)** *Zostera japonica* seagrass habitats along the coastal topographic gradient in the Yellow River Delta. Abbreviations for the trophic groups: Biv, bivalves; Ca, *Carassius auratus*; Cra, crabs; Gas, gastropods; Ins, Insects; Lj, *Lateolabrax japonicus*; Mic, microphytobenthos; OtC, other crustaceans; Pa, *Phragmites australis*; Ph, *Planiliza haematocheila*; Phy, phytoplankton; Pol, polychaetes; POM, particulate organic matter; Sa, *Spartina alterniflora*; Sh, *Synechogobius hasta*; Shr, shrimp; SOM, sediment organic matter, Ss, *Suaeda salsa*; Zj, *Zostera japonica*; Zoo, zooplankton.

The consumer δ^{15}N values also differed significantly (for the *P. australis* habitat, $F_{7,44} = 6.16$, $p < 0.001$; for the *S. salsa* habitat, $F_{9,68} = 40.24$, $p < 0.001$; for the *S. alterniflora* habitat, $F_{10,88} = 10.06$, $p < 0.001$; for the *Z. japonica* habitat, $F_{10,83} = 14.93$, $p < 0.001$). In the *P. australis* habitat, the δ^{15}N values of other crustaceans (2.66 ± 0.72‰) and gastropods (3.31 ± 0.77‰) were significantly lower than those of the fish ($p < 0.001$), which were 8.58 ± 2.94‰ and 8.48 ± 1.99‰ for *Planiliza haematocheila* and *Synechogobius hasta*, respectively. In the *S. salsa*, *S. alterniflora*, and *Z. japonica* habitats, *Lateolabrax japonicus* had the highest δ^{15}N values, and the difference from other groups was often significant. In the *S. salsa* habitat, *P. haematocheila* had significantly higher δ^{15}N values (9.38 ± 1.32‰) than zooplankton (5.63 ± 1.32‰), bivalves (5.59 ± 0.90‰), gastropods (6.48 ± 0.90‰), other crustaceans (5.54 ± 0.47‰), and crabs (5.80 ± 1.89‰) ($p < 0.05$). In the *S. alterniflora* habitat, *S. hasta* had a significantly ($p < 0.05$) higher δ^{15}N value (10.95 ± 0.80‰) than zooplankton (6.46 ± 1.39‰), bivalves (7.29 ± 0.94‰), and crabs (7.47 ± 1.71‰). In addition, *P. haematocheila*, *Carassius auratus*, and *S. hasta* in the *Z. japonica* habitat all had significantly higher δ^{15}N values than the zooplankton and macroinvertebrates, except for gastropods, crabs, and polychaetes.

Trophic Positions of Consumer Trophic Groups

We determined the trophic positions of consumer trophic groups based on their δ^{15}N values relative to a baseline that equaled the average value of all detritivores and herbivores for each habitat. The highest trophic position of consumer trophic groups in the *S. salsa* habitat (3.92) was slightly higher than the highest position in the *Z. japonica* habitat (3.62), followed by the *S. alterniflora* (3.32) and *P. australis* (3.25) habitats (**Figure 3**). Trophic positions of zooplankton, bivalves, gastropods, *C. auratus*, *S. hasta*, and *L. japonicus* all differed significantly among the four habitats ($p < 0.05$). Specifically, zooplankton had a higher trophic position in the *P. australis* habitat (2.41 ± 0.43) than in other habitats, at 1.94 ± 0.42 in the *S. salsa* habitat, 1.65 ± 0.46 in the *S. alterniflora* habitat, and 1.76 ± 0.62 for the *Z. japonica* habitat. In the *Z. japonica* habitat, bivalves (2.28 ± 0.27), gastropods (2.60 ± 0.40), and *C. auratus* (3.42 ± 0.37) all had significantly higher trophic positions than in the other habitats ($p < 0.05$). The trophic positions of *S. hasta* and *L. japonicus* were both highest in the *S. salsa* habitat (3.58 ± 0.14 and 3.94 ± 0.22, respectively), followed by the *Z. japonica* habitat (3.44 ± 0.13 and 3.62 ± 0.41, respectively), and were lowest in the *S. alterniflora* habitat (3.08 ± 0.26 and 3.32 ± 0.30, respectively).

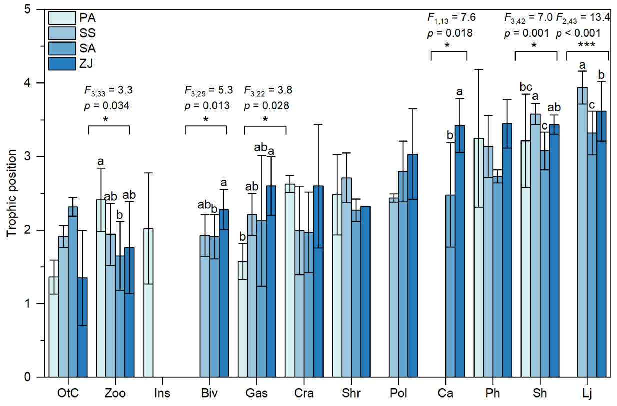

FIGURE 3 | Trophic positions (mean ± SD) identified based on the δ^{15}N values of consumer trophic groups collected from the *Phragmites australis* (PA), *Suaeda salsa* (SS), *Spartina alterniflora* (SA), and *Zostera japonica* seagrass (ZJ) habitats along the coastal topographic gradient in the Yellow River Delta wetland. Abbreviations for the trophic groups: Biv, bivalves; Ca, *Carassius auratus*; Cra, crabs; Gas, gastropods; Ins, Insects; Lj, *Lateolabrax japonicus*; OtC, other crustaceans; Ph, *Planiliza haematocheila*; Pol, polychaetes; Sh, *Synechogobius hasta*; Shr, shrimp; Zoo, zooplankton. The position of consumers on the x-axis from left to right represents an increase in the mean trophic position of the consumers across the four habitats. Significant differences in the trophic positions of the consumers among the four habitats were evaluated by one-way ANOVA (*p < 0.05; ***p < 0.001). Bars for a given trophic group that are labeled with different letters differ significantly (Tukey's HSD test, p < 0.05).

Trophic Diversity of Trophic Groups

The corrected standard ellipse areas (SEA_c) for different assemblages across the four habitats were calculated by SIBER analysis to identify their relative trophic diversity (**Figure 4 and Supplementary Table 6**). SEA_c ellipses for the carbon sources, all consumers combined, and individual consumer trophic groups differed among the four habitats in size, shape, and position in the δ^{13}C vs. δ^{15}N plots, which suggested that some trophic groups had shifted their trophic niche along the coastal topographic gradient. In the *S. alterniflora* and *Z. japonica* habitats, the positions of the SEA_c ellipses for the carbon sources, all consumers combined, gastropods, and *S. hasta* showed higher δ^{13}C and δ^{15}N values than in the *P. australis* and *S. salsa* habitats (**Figures 4A, B, E, I**). In addition, the SEA_c of bivalves and crabs showed higher δ^{15}N values in the *S. alterniflora* and *Z. japonica* habitats than in the *S. salsa* habitat (**Figures 4D, F**).

Regarding the size of SEA_c, *S. alterniflora* habitat had the smallest SEA_c for both carbon sources (11.32‰^{2}) and all consumers combined (25.86‰^{2}) (**Figure 4 and Supplementary Table 6**). Specifically, for zooplankton, SEA_c was largest in the *S. salsa* habitat (22.51‰^{2}) and smallest in the *S. alterniflora* habitat (4.91‰^{2}). Bivalves and crabs gradually had larger SEA_c from the *S. salsa* habitat to the *S. alterniflora* and *Z. japonica* habitats. Gastropods had the largest SEA_c in the *S. alterniflora* (27.41‰^{2}), followed by the *Z. japonica* habitat (13.62‰^{2}), with lower values in the *P. australis* and *S. salsa* habitats (< 9‰^{2}). *P. haematocheila* and *S. hasta* both had the largest SEA_c in the *P. australis* habitat (22.90‰^{2} and 10.41‰^{2}, respectively), whereas *C. auratus* had the largest SEA_c in the *S. alterniflora* habitat (29.08‰^{2}). Variation of SEA_c of *L. japonicus* among the four habitats was small, with values ranging from 1.53‰^{2} to 4.47‰^{2}.

Supplementary Table 7 summarizes the overlaps of the ellipses among the four sites. Trophic groups showed high overlaps among the four habitats (**Figure 4**), with overlaps ranging from 24.5% to 60.0% for the carbon sources, and from 27.7 to 81.5% for all consumers combined. In addition, only the overlaps for zooplankton between the *P. australis* and *S. alterniflora* habitats and for bivalves between the *S. salsa* and *Z. japonica* habitats were lower than 6%.

Layman's community metrics also varied across habitats, but with strongly different patterns (**Figure 5**). *CR*, *TA*, and *CD* showed similar patterns across the four habitats, with their highest values in the *S. salsa* habitat, followed by the *P. australis* or *Z. japonica* habitat, and the lowest values in the *S. alterniflora* habitat. This contrasts with the *NR* metric, which was lowest in the *S. salsa* habitat and highest in the *S. alterniflora* habitat. *MNND* was highest in the *S. salsa* habitat, followed by the *P. australis* and *S. alterniflora* habitats, but lowest in the *Z. japonica* habitat. Whereas *SDNND* was highest in the *Z. japonica* habitat, followed by the *S. salsa* habitat, and lowest in the *P. australis* habitat.

Food Web Trophic Structure and Topological Properties

The SIAR modeling revealed high variability in the diet compositions of the consumer trophic groups across the four habitats (**Figure 6**), except for insects, shrimps, and polychaetes. Diagrams of the trophic structure of these food webs were shown in **Supplementary Figures 1–4**. The diet composition of zooplankton was relatively evenly distributed in the *P. australis* and *Z. japonica* habitats, with POM and phytoplankton accounting for 60% and 40% in the *P. australis* habitat, and 54% and 46% in the *Z. japonica* habitat, respectively. Whereas zooplankton relied almost exclusively on phytoplankton (ca. 83%) in both the *S. salsa* and *S. alterniflora* habitats. Bivalves showed a slight dietary preference for phytoplankton (61%) in the *S. salsa* habitat, but depended on POM (59%) in the *Z. japonica* habitat. Bivalves had a particularly high preference for POM (89%) in the *S. alterniflora* habitat. Gastropods had relatively evenly distributed diet compositions, with the highest contribution by *P. australis* (37%) in the *P. australis* habitat. In the other three habitats, gastropods mostly relied on SOM (53, 47, and 44% for the *S. salsa*, *S. alterniflora*, and *Z. japonica* habitats, respectively), followed by *S. alterniflora* (32%) in the *S. alterniflora* habitat and microphytobenthos in the *S. salsa* and *Z. japonica* habitats (ca. 30%). A range of prey contributed to the diet of crabs in these four habitats, with the highest contribution of 24% from *P. australis* in the *P. australis* habitat, ca. 19% from SOM in the *S. salsa* and *Z. japonica* habitats, and 24% from POM in the *S. alterniflora* habitat. Large differences were evident in the dietary composition of the other crustaceans across the four habitats; they relied substantially on POM in the *P. australis* habitat (85%) and *S. alterniflora* habitat

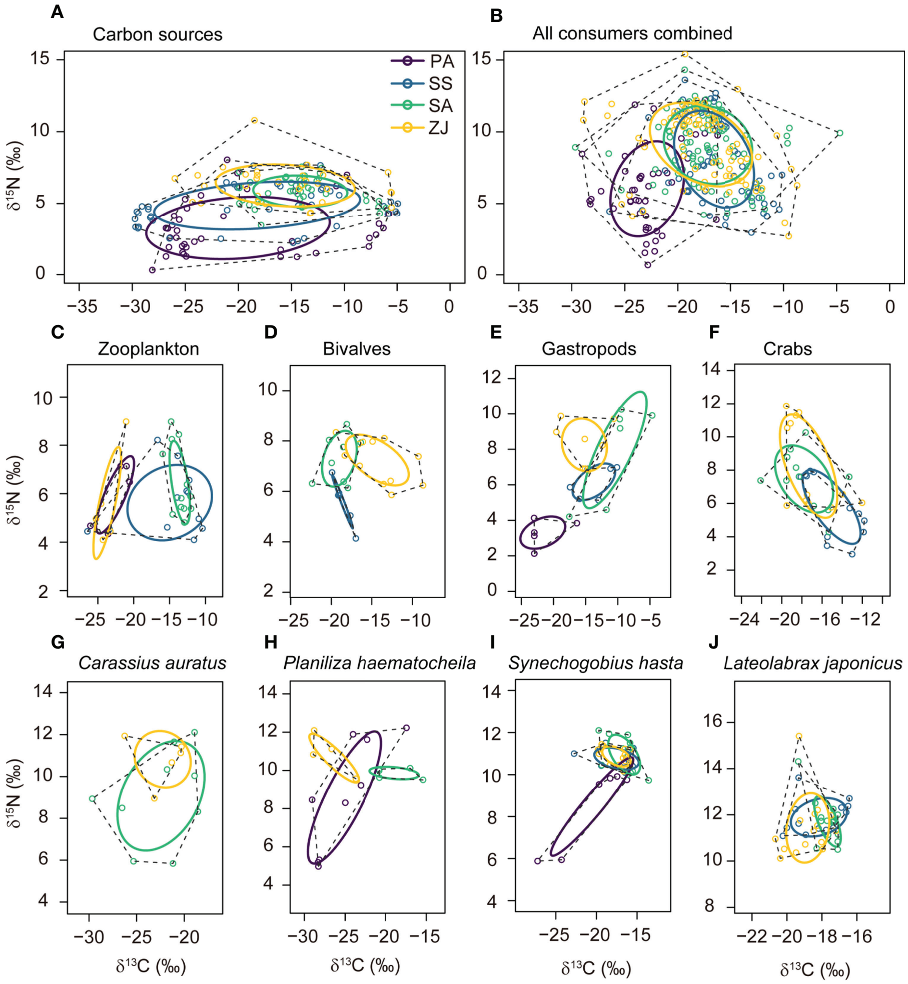

FIGURE 4 | Corrected standard niche ellipses (solid lines) and convex hulls (dashed lines) for the isotope-based niche areas of **(A)** the carbon sources, consisting of detritus and primary producers; **(B)** all consumers combined; and **(C-J)** individual consumer trophic groups for the *Phragmites australis* (PA), *Suaeda salsa* (SS), *Spartina alterniflora* (SA), and seagrass *Zostera japonica* seagrass (ZJ) habitats along the coastal topographic gradient in the Yellow River Delta wetland. Graphs were produced using the SIBER package implemented in the R software. Each point shows the δ^{13}C and δ^{15}N values for a sample, with colors based on the habitat where this data was collected. The ellipses, hulls, and data points for a given consumer trophic group collected in a given habitat in **(C)** to **(J)** are only provided when the sample size is ≥ 5.

(63%), but only approximately 50% on both SOM and POM in the *S. salsa* and *Z. japonica* habitats.

The fish *P. haematocheila*, *C. auratus*, and *S. hasta* all had broad diet compositions, with no dominant prey. However, microphytobenthos accounted for 38% of the diet of *C. auratus*, and *S. hasta* preferred polychaetes and shrimp in the *S. salsa* habitat but zooplankton and crabs in the *S. alterniflora* habitat. *L. japonicus* had obvious diet preferences across these habitats; it preferred shrimps (46%) and *S. hasta* (30%) in the *S. salsa* habitat, shrimps (41%) and crabs (27%) in the *S. alterniflora* habitat, and all three prey (ranging from 20 to 26%) in the *Z. japonica* habitat.

We observed clear differences among the four habitats in the food web topological properties (**Table 1**). *S*, *L*, *LD*, *I*, and *O* were all higher in the *S. alterniflora* and *Z. japonica* habitats than in the *S. salsa* habitat, and were lowest in the *P. australis* habitat. In contrast, *C*, *T*, *B*, and *MaxSim* showed the opposite pattern, though the differences were very small.

DISCUSSION

Despite the challenges in resolving empirical coastal food webs on a large scale, this study disentangled the spatial variation of the trophic diversity of trophic groups and the structure of the entire food web across variable vegetated habitats along a coastal topographic gradient in the Yellow River Delta. Our two initial hypotheses were both confirmed. Specifically, the measured stable isotope ratios of the trophic groups, the trophic positions of consumers, the isotopically defined trophic diversity, the quantitative diet compositions, and the topological properties all varied markedly along the coastal

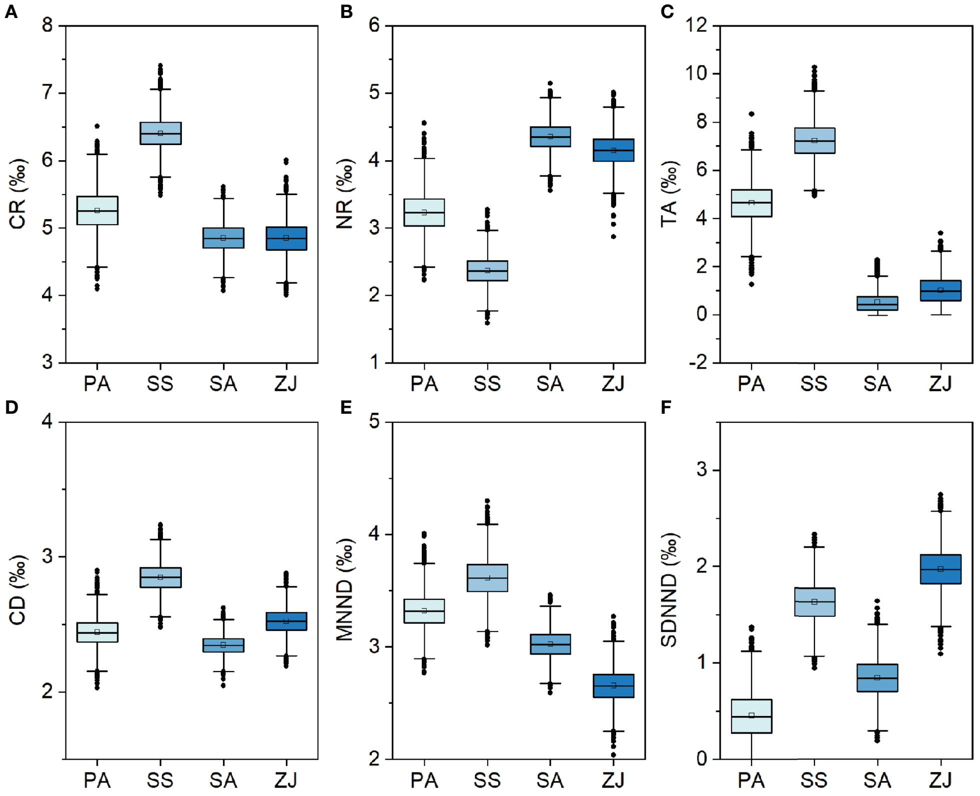

FIGURE 5 | Boxplots representing Bayesian model estimates for six Layman community metrics: **(A)** the δ^{13}C range (*CR*), **(B)** the δ^{15}N range (*NR*), **(C)** the total area (*TA*), **(D)** the mean distance to the centroid (*CD*), **(E)** the mean nearest-neighbor distance (*MNND*), and **(F)** the standard deviation of the nearest-neighbor distance (*SDNND*) across the *Phragmites australis* (PA), *Suaeda salsa* (SS), *Spartina alterniflora* (SA), and *Zostera japonica* seagrass (ZJ) habitats along the coastal topographic gradient in the Yellow River Delta wetland.

topographic gradient. However, we found no consistent trend for multiple metrics of trophic diversity and trophic structure. It is worth noting that trophic groups in the habitat dominated by invasive *S. alterniflora* mostly had rather low values of isotopically defined trophic diversity. The seaside habitats had higher values of food web topological properties than the higher-elevation habitats in terms of species richness, number of trophic links, and linkage density; that is, they had more complex food webs.

Spatial Variability in Trophic Diversity of the Trophic Groups Along the Topographic Gradient

Our measured δ^{13}C values for the carbon sources in the four habitats were similar to those that were previously reported for temperate estuarine and coastal ecosystems in other parts of the world (Bristow et al., 2013; Park et al., 2017; Kim et al., 2020). However, our δ^{13}C value for *Z. japonica* seagrass (-13.8 ± 0.3‰) was slightly lower than that for the same species along the Gudong embankment in the Yellow River Delta's coastal wetland (-11.7 ± 0.4‰) (Li et al., 2021) and lower than the range in a review of 31 studies in seagrass ecosystems (-10 to -11‰) (Hemminga and Mateo, 1996), but approached the values (-10.1 to 14.0‰) in some temperate seagrass beds (e.g., Hanson et al., 2010; Mittermayr et al., 2014). We found that the C4 plants of *S. alterniflora* and *Z. japonica* seagrass were significantly more ^{13}C-enriched than the C3 plants of *P. australis* and *S. salsa*, probably due to their different photosynthetic pathways (Peterson and Fry, 1987). SOM was more ^{13}C-enriched than POM in all four habitats, which is consistent with a previously reported separation between pelagic and benthic carbon sources (Kiljunen et al., 2020). However, our comparisons between pelagic algae (i.e., phytoplankton) and benthic algae (i.e., microphytobenthos) tended to be confused among the four habitats. That is, phytoplankton were more ^{13}C-depleted than microphytobenthos in both *P. australis* and *Z. japonica* habitats, but less ^{13}C-depleted in the *S. salsa* and *S. alterniflora* habitats.

The phytoplankton δ^{13}C values (ca. -15‰) in the *S. salsa* and *S. alterniflora* habitats were lower than the values commonly observed in temperate waters (-22 to -20‰; Cresson et al., 2012). We hypothesize that our conservative estimates for the phytoplankton stable isotope signatures in the two habitats were either influenced by water salinity and dissolved inorganic carbon (Careddu et al., 2015) or due to the fact that the collected phytoplankton may reflect a combination of phytoplankton, microorganisms, and POM of undefined origins (Young et al., 2021). The lower δ^{13}C values for SOM in the higher-elevation *P. australis* habitat compared with the

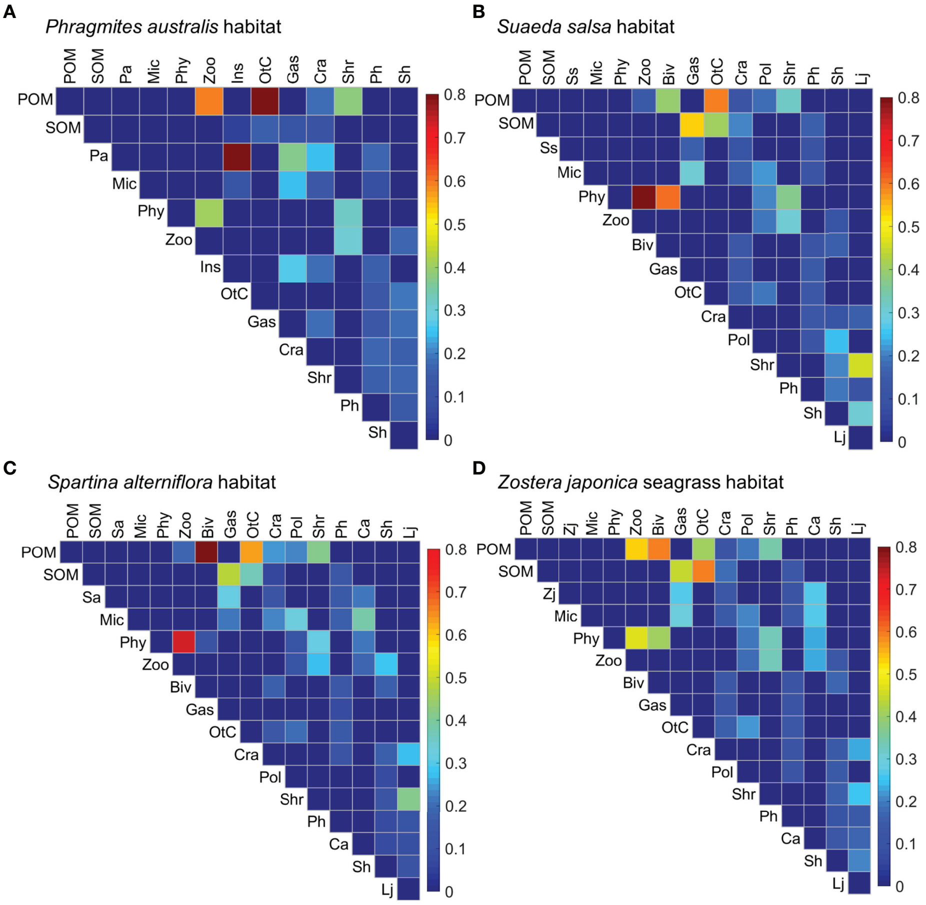

FIGURE 6 | Diet compositions for each trophic group (in the columns) foraging on its prey (in the rows) in the **(A)** *Phragmites australis*, **(B)** *Suaeda salsa*, **(C)** *Spartina alterniflora*, and **(D)** *Zostera japonica* seagrass habitats along the coastal topographic gradient in the Yellow River Delta wetland. Color intensity is proportional to the magnitude of the diet contributions of the prey to the consumer trophic groups. Abbreviations for the trophic groups: Abbreviations for the trophic groups: Biv, bivalves; Ca, *Carassius auratus*; Cra, crabs; Gas, gastropods; Ins, Insects; Lj, *Lateolabrax japonicus*; Mic, microphytobenthos; OtC, other crustaceans; Pa, *Phragmites australis*; Ph, *Planiliza haematocheila*; Phy, phytoplankton; Pol, polychaetes; POM, particulate organic matter; Sa, *Spartina alterniflora*; Sh, *Synechogobius hasta*; Shr, shrimp; SOM, sediment organic matter, Ss, *Suaeda salsa*; Zj, *Zostera japonica*; Zoo, zooplankton.

TABLE 1 | Topological properties of the food webs in the *Phragmites australis* (PA), *Suaeda salsa* (SS), *Spartina alterniflora* (SA), and *Zostera japonica* seagrass (ZJ) habitats along the coastal topographic gradient in the Yellow River Delta.

Metrics	Definitions	PA	SS	SA	ZJ
Richness (*S*)	Number of trophic groups in the food web	13	15	16	16
Links (*L*)	Number of trophic links between the trophic groups	33	42	46	48
Linkage density (*LD*)	$LD = L/S$	2.54	2.80	2.88	3.00
Connectance (*C*)	$C= L/S^2$	0.20	0.19	0.18	0.19
Top species (*T*)	Proportion of species that have no predators	0.08	0.07	0.06	0.06
Intermediate species (*I*)	Proportion of species that have both prey and predators	0.54	0.60	0.63	0.63
Basal species (*B*)	Proportion of species that have no prey	0.38	0.33	0.31	0.31
Omnivory (O)	Proportion of species that consume prey from more than one trophic level	0.38	0.40	0.44	0.44
GenSD	Standard deviation of the number of resources per species	2.57	2.70	2.55	2.76
VulSD	Standard deviation of the number of consumers per species	1.27	1.42	1.71	1.59
ATL	Average trophic level	1.77	1.90	1.90	1.91
MaxSim	Maximum Jaccardian similarity	0.65	0.59	0.57	0.58

Metrics with values that increased along the gradient are boldfaced.

lower-elevation *S. alterniflora* and *Z. japonica* habitats are consistent with the findings of Park et al. (2017), and are also consistent with observations that the $\delta^{13}C$ values of POM in freshwater are significantly lower than those in saltwater (Dibble and Meyerson, 2014; Ye et al., 2017). The microphytobenthos $\delta^{13}C$ values in the *P. australis* and *Z. japonica* habitats (ca. -15‰) were slightly higher than those in the *S. salsa* and *Z. japonica* habitats (ca. -19‰), but were comparable with the range (-14.8 ± 0.8‰) reported in coastal wetlands (Kim et al., 2020).

The overall $\delta^{13}C$ range of the consumers collected from the *P. australis* habitat was narrow and the values were lower than those in the other three habitats, possibly reflecting the carbon isotopic signatures of the dominant primary producer (Wozniak et al., 2006). Similarly, Park et al. (2015) showed that the $\delta^{13}C$ values of consumers in *P. australis* habitat were lower than those in the *Suaeda japonica* habitat. Garcia et al. (2018) showed an overall increasing trend in mean consumer $\delta^{13}C$ values along a river–estuary–surf zone transect. Higher consumer $\delta^{15}N$ values were found in the seaside habitats (i.e., the *S. salsa*, *S. alterniflora*, and *Z. japonica* habitats) than in the *P. australis* habitat, which is in line with the findings of Kim et al. (2020). The highest trophic position for all consumers combined was observed in the *S. salsa* habitat, followed by the *Z. japonica* habitat, and was lower in the *S. alterniflora* and *P. australis* habitats. The trophic positions are comparable to the value (3.76) for the highest trophic position reported in the lower reaches of the Yangtze River (Mao et al., 2016). We found the highest trophic position for the sea bass, *L. japonicus*, in the *S. salsa*, *S. alterniflora*, and *Z. japonica* habitats, which is consistent with recent studies showing that *L. japonicus* is a typical top predator in China's coastal and offshore waters (Islam et al., 2011; Li et al., 2021). It is worth noting that the four fish species, as well as the zooplankton, bivalves, crabs, and shrimps, had the lowest average trophic positions in the habitat dominated by the invasive *S. alterniflora* habitat. Thus, we hypothesize that *S. alterniflora*, despite its dense distribution pattern and high biomass, transferred less primary productivity to higher trophic levels. This is might because consumers rarely ingest *S. alterniflora* directly (Wittyngham, 2021). In addition, *S. alterniflora* detritus is largely buried in sediments as plant-derived carbon affected by the decomposition of microorganisms or washed to adjacent coasts due to tidal dynamics, which both imply that its production is rarely recycled to higher trophic levels (Yan et al., 2019; Zhang et al., 2021).

Based on the trophic diversity revealed by the SIBER analysis, the habitat dominated by invasive *S. alterniflora* showed weak ecosystem functioning, as it had the lowest SEA_c, CR, TA, and CD values for carbon sources and for all consumers combined. This suggests that there was a low separation in $\delta^{13}C$ values among carbon sources in the habitat, and that consumers tended to have similar niche signatures (Abrantes et al., 2014). Similarly, Feng et al. (2018) found that communities in *S. alterniflora* habitat had lower SEA_c than natural mangrove forests, indicating significant resource competition among different consumers in the *S. alterniflora* habitat.

We observed a large overlap among the ellipses for all consumers combined in the *S. salsa*, *S. alterniflora*, and *Z. japonica* habitats, indicating high competition in resource utilization among consumers in the three habitats. In contrast, consumers in these three habitats overlapped less with the *P. australis* habitat, suggesting a large habitat heterogeneity between the *P. australis* habitat and the three habitats. This is probably mainly due to the composition of the macroinvertebrate consumers, which were dominated by insects in the *P. australis* habitat, but were dominated by bivalves, gastropods, and polychaetes in the *S. salsa*, *S. alterniflora*, *Z. japonica* habitats due to their living habits in brackish water and saltwater (Dauer et al., 2010; Li et al., 2020).

Habitat Heterogeneity Created Highly Variable Food Webs Along the Topographic Gradient

Though insects, shrimps, and polychaetes showed little variation across the four habitats, other consumers and the overall food web trophic structure displayed high variation based on the SIAR analysis. Zooplankton showed a much higher reliance on phytoplankton in the *S. alterniflora* and *Z. japonica* habitats than in the *P. australis* and *S. salsa* habitats, indicating that the *S. alterniflora* and *Z. japonica* habitats are strongly influenced by nutrition imports from the adjacent marine ecosystem (Heck et al., 2008). Bivalves, as typical filter-feeding organisms, showed dietary preferences for POM and phytoplankton, which is consistent with previous studies (Atkinson et al., 2014; Li et al., 2021). Gastropods showed a slight preference for direct feeding on *P. australis*, *S. salsa*, and seagrass, but ca. 32% of the diet was *S. alterniflora*. Similarly, Feng et al. (2014) found that gastropods in a *Spartina* wetland derived more than 80% of their organic carbon from *Spartina*. In agreement with previous studies (Evrard et al., 2012; Kim et al., 2020), we also found that gastropods relied greatly on SOM and the microphytobenthos. Unfortunately, we did not sample epiphytes attached to plant leaves, which have been determined to be one of the main energy providers to gastropods, especially in seagrass meadows (Cook et al., 2011; Voigt and Hovel, 2019). Crabs showed highly generalist feeding in the Yellow River Delta coastal wetland, as they fed on both pelagic and benthic carbon sources, as well as on detritus and primary producers. Together with their high abundance in coastal wetlands, crabs are a key component of coastal food webs, and their trophic interactions play a fundamental role in maintaining food web stability (Vermeiren et al., 2015; Hoy et al., 2019).

Since we defined a trophic group as a species cluster that shares the same prey and predators, we considered less complex food webs than in some previous studies conducted in estuarine and coastal wetlands (Vinagre and Costa, 2014; Careddu et al., 2015; Mendonça et al., 2018). Despite the small variation in the number of trophic groups, we found that other topological properties differed along the topographic gradient. The linkage density values of the four habitats (2.54 to 3.00) were lower than previously reported values (ca. 2.5 to 3.8) in an estuary–coastal system (Vinagre and Costa, 2014) and some other aquatic ecosystems (Mor et al., 2018; Kortsch et al., 2019), but fell with the range (1.6 to 25.1) for empirical food webs reported by Dunne et al. (2002). We found that our seaside habitats had higher values of the topological metrics than the higher-elevation habitats, similarly, Vinagre and Costa (2014) found upper estuary had the lowest values of linkage density than habitats in the lower estuary. The proportion of omnivorous consumers in our study ranged from 38 to 44%, which was much higher than the values (11 to 20%) reported in a riverine ecosystem (Mor et al., 2018) and (11 to 39%) in intertidal pools (Mendonça et al., 2018), but lower than the reported range (45 to 65%) for estuarine wetlands (Vinagre and Costa, 2014).

Implications for Coastal Wetland Conservation and Management

Recent research on food web changes along a coastal topographic gradient has been scarce (e.g., Robson et al., 2017) compared to the number conducted along variable environmental gradients in riverine ecosystems (Mor et al., 2018), lacustrine ecosystems (van der Lee et al., 2021), and marine ecosystems (Kortsch et al., 2015; Nordström and Bonsdorff, 2017). This is an important research gap, since coastal wetlands display significant variations in environmental factors and biological signatures such as the community composition, species stress tolerance, and trophic niche width. Thus, the heterogeneous habitats should create highly variable food web characteristics along coastal environmental or geographic gradients, which agrees with the results of our study. With the intensification of human coastal activities such as seashore reclamation, ditch diversion, and aquaculture, the habitat heterogeneity of coastal wetland has been both, directly and indirectly, decreased, leading to a decrease in species taxonomic and functional diversity, and ultimately resulting in a more homogeneous ecosystem with relatively similar food web attributes (Feit et al., 2019; Li et al., 2019). This will ultimately pose a major threat to biodiversity conservation, ecosystem functions, and the maintenance of ecosystem resilience (Thrush et al., 2008; Lohrer et al., 2015).

The invasive species *S. alterniflora* showed relatively weak ecosystem functions compared with the adjacent communities of native *S. salsa* and seagrass, especially in terms of the trophic positions of consumers and the isotopically defined trophic diversity. This suggests that *S. alterniflora* wetland has not formed a healthy ecosystem and has not effectively performed ecosystem functioning, even though the invasion began about 10 years before our study. Given the rapid expansion of this species, with its area increasing by 50,204 ha during the past 25 years along the Chinese coastline (Mao et al., 2019), our results suggest that more protective measures should be taken to limit its spread and thereby protect or enhance the function of coastal ecosystems. Recently, many studies have tried to identify the effects of the invasion by *S. alterniflora* to better control and remove the species (Ainouche and Gray, 2016; Meng et al., 2020). Unfortunately, managing this species at an ecosystem scale has proven difficult (Wails et al., 2021). Further studies will be needed to investigate how ecosystem functions such as energy transfer efficiency and ecosystem stability are affected by the *S. alterniflora* invasion. The results should provide new insights that will lead to the development of more effective management strategies with practical and attainable goals.

CONCLUSIONS

In this study, we combined the isotopically defined trophic diversity from the SIBER analysis with the quantitative trophic structure from the SIAR analysis to investigate the spatial variation of empirically resolved food webs across variable vegetated habitats along a coastal topographic gradient. Although we didn't reveal a continuous overall trend for changes in the food web characteristics due to inconsistent trends for different metrics of trophic diversity and structure, we nonetheless observed that the δ^{13}C values of the carbon sources and the δ^{15}N values of the consumers were both higher in the seaside habitats than in the higher-elevation habitats. The habitat dominated by invasive *S. alterniflora* had the lowest values for most metrics in the SIBER analysis, indicating weak ecosystem functioning in terms of the trophic niche characteristics. The relative diet contributions for the consumers varied greatly among the four habitats, except for shrimps and polychaetes. The complexity of the food webs increased along the gradient from upland to near-shore habitats in terms of the species richness, the number of trophic links, and the linkage density. In addition, the proportions of intermediate consumers and omnivores and the average trophic level also increased along this gradient. Overall, we found that habitat heterogeneity formed highly variable food webs along the topographic gradient. This knowledge will enhance our ability to protect the coastal habitat heterogeneity, which plays a decisive role in maintaining biodiversity and ecosystem functions. Based on our results, we propose that more attention should be paid to the habitat dominated by invasive *S. alterniflora* in China's coastal wetlands, and that adaptive and effective management should be implemented at an ecosystem scale to mitigate the impacts of this invasion.

DATA AVAILABILITY STATEMENT

The original contributions presented in the study are included in the article/supplementary material. Further inquiries can be directed to the corresponding authors.

AUTHOR CONTRIBUTIONS

XL and WY conceived the original idea and designed the study. XL performed the field sampling and data analysis under the joint supervision of WY, TS, and ZY. XL wrote the first draft of the manuscript. All authors contributed to manuscript revision, and have read and approved the manuscript for submission.

FUNDING

This study was financially supported by the Joint Funds of the National Natural Science Foundation of China (U1806217), the Program for Guangdong Introducing Innovative and Entrepreneurial Teams (2019ZT08L213), the Key Special Project for Introduced Talents Team of Southern Marine Science and Engineering Guangdong Laboratory (Guangzhou) (GML2019ZD0403), and the Guangdong Provincial Key Laboratory Project (2019B121203011).

ACKNOWLEDGMENTS

We are indebted to Jun Pei, Ziyue Zhang, and Xianting Fu for invaluable field assistance. We also thank Geoffrey Hart for providing language help during the writing of this paper.

SUPPLEMENTARY MATERIAL

The Supplementary Material for this article can be found online at: https://www.frontiersin.org/articles/10.3389/fmars.2022.920745/full#supplementary-material

REFERENCES

Abrantes, K. G., Barnett, A., and Bouillon, S. (2014). Stable Isotope-Based Community Metrics as a Tool to Identify Patterns in Food Web Structure in East African Estuaries. *Funct. Ecol.* 28 (1), 270–282. doi: 10.1111/1365-2435.12155

Ainouche, M., and Gray, A. (2016). Invasive *Spartina*: Lessons and Challenges. *Biol. Invas.* 18 (8), 2119–2122. doi: 10.1007/s10530-016-1201-7

Atkinson, C. L., Kelly, J. F., and Vaughn, C. C. (2014). Tracing Consumer-Derived Nitrogen in Riverine Food Webs. *Ecosystems* 17, 485–496. doi: 10.1007/s10021-013-9736-2

Baiser, B., Gravel, D., Cirtwill, A. R., Dunne, J. A., Fahimipour, A. K., Gilarranz, L. J., et al. (2019). Ecogeographical Rules and the Macroecology of Food Webs. *Global Ecol. Biogeogr.* 28, 1204–1218. doi: 10.1111/geb.12925

Baker, R., Abrantes, K., and Feller, I. C. (2021). Stable Isotopes Suggest Limited Role of Wetland Macrophyte Production Supporting Aquatic Food Webs Across a Mangrove-Salt Marsh Ecotone. *Estuar. Coast.* 44, 1619–1627. doi: 10.1007/s12237-021-00895-5

Bang, J. H., Bae, M. J., and Lee, E. J. (2018). Plant Distribution Along an Elevational Gradient in a Macrotidal Salt Marsh on the West Coast of Korea. *Aquat. Bot.* 147, 52–60. doi: 10.1016/j.aquabot.2018.03.005

Barbier, E. B., Hacker, S. D., Kennedy, C., Koch, E. W., Stier, A. C., and Silliman, S. B. R. (2011). The Value of Estuarine and Coastal Ecosystem Services. *Ecol. Monogr.* 81, 169–193. doi: 10.1890/10-1510.1

Bentivoglio, F., Calizza, E., Rossi, D., Carlino, P., Careddu, G., Rossi, L., et al. (2016). Site-Scale Isotopic Variations Along a River Course Help Localize Drainage Basin Influence on River Food Webs. *Hydrobiologia* 770, 257–272. doi: 10.1007/s10750-015-2597-2

Bristow, L. A., Jickells, T. D., Weston, K., Marca-Bell, A., Parker, R., and Andrews, J. E. (2013). Tracing Estuarine Organic Matter Sources Into the Southern North Sea Using C and N Isotopic Signatures. *Biogeochemistry* 113, 9–22. doi: 10.1007/s10533-012-9758-4

Cardona, L., Lloret-Lloret, E., Moles, J., and Avila, C. (2021). Latitudinal Changes in the Trophic Structure of Benthic Coastal Food Webs Along the Antarctic Peninsula. *Mar. Environ. Res.* 167, 105290. doi: 10.1016/j.marenvres.2021.105290

Careddu, G., Costantini, M. L., Calizza, E., Carlino, P., Bentivoglio, F., Orlandi, L., et al. (2015). Effects of Terrestrial Input on Macrobenthic Food Webs of Coastal Sea are Detected by Stable Isotope Analysis in Gaeta Gulf. *Estuar. Coast. Shelf. Sci.* 154, 158–168. doi: 10.1016/j.ecss.2015.01.013

Christianen, M. J. A., Middelburg, J. J., Holthuijsen, S. J., Jouta, J., Compton, T. J., van der Heide, T., et al. (2017). Benthic Primary Producers are Key to Sustain the Wadden Sea Food Web: Stable Carbon Isotope Analysis at Landscape Scale. *Ecology* 98, 1498–1512. doi: 10.1002/ecy.1837

Colombano, D. D., Litvin, S. Y., Ziegler, S. L., Alford, S. B., Baker, R., Barbeau, M. A., et al. (2021). Climate Change Implications for Tidal Marshes and Food Web Linkages to Estuarine and Coastal Nekton. *Estuar. Coast.* 44, 1637–1648. doi: 10.1007/s12237-020-00891-1

Cook, K., Vanderklift, M. A., and Poore, A. G. B. (2011). Strong Effects of Herbivorous Amphipods on Epiphyte Biomass in a Temperate Seagrass Meadow. *Mar. Ecol. Progr. Ser.* 442, 263–269. doi: 10.3354/meps09446

Cresson, P., Ruitton, S., Fontaine, M. F., and Harmelin-Vivien, M. (2012). Spatio-Temporal Variation of Suspended and Sedimentary Organic Matter Quality in the Bay of Marseilles (NW Mediterranean) Assessed by Biochemical and Isotopic Analyses. *Mar. Pollut. Bull.* 64 (6), 1112–1121. doi: 10.1016/j.marpolbul.2012.04.003

Cui, B. S., He, Q., and An, Y. (2011). Community Structure and Abiotic Determinants of Salt Marsh Plant Zonation Vary Across Topographic Gradients. *Estuar. Coast.* 34, 459–469. doi: 10.1007/s12237-010-9364-4

Dauer, D. M., Ewing, R. M., and Rodi, A. J.Jr. (2010). Macrobenthic Distribution Within the Sediment Along an Estuarine Salinity Gradient. *Internat. Rev. Hydrobiol.* 72, 529–538. doi: 10.1002/iroh.19870720502

Dibble, K. L., and Meyerson, L. A. (2014). The Effects of Plant Invasion and Ecosystem Restoration on Energy Flow Through Salt Marsh Food Webs. *Estuar. Coast.* 37, 339–353. doi: 10.1007/s12237-013-9673-5

Dunne, J. A., Williams, R. J., and Martinez, N. D. (2002). Food-Web Structure and Network Theory: The Role of Connectance and Size. *Proc. Natl. Acad. Sci. U.S.A.* 99, 12917–12922. doi: 10.1073/pnas.192407699

Engels, J. G., Rink, F., and Jensen, K. (2011). Stress Tolerance and Biotic Interactions Determine Plant Zonation Patterns in Estuarine Marshes During Seedling Emergence and Early Establishment. *J. Ecol.* 99, 277–287. doi: 10.1111/j.1365-2745.2010.01745.x

Evrard, V., Huettel, M., Cook, P. L. M., Soetart, K., and Middelburg, J. J. (2012). Importance of Phytodetritus and Microphytobenthos for Heterotrophs in a Shallow Subtidal Sandy Sediment. *Mar. Ecol. Progr. Ser.* 455, 13–31. doi: 10.3354/meps09676

Feit, B., Blüthgen, N., Traugott, M., and Jonsson, M. (2019). Resilience of Ecosystem Processes: A New Approach Shows That Functional Redundancy of Biological Control Services is Reduced by Landscape Simplification. *Ecol. Lett.* 22, 1568–1577. doi: 10.1111/ele.13347

Feng, J. X., Guo, J. M., Huang, Q., Jiang, J. X., Huang, G. M., Yang, Z. W., et al. (2014). Changes in the Community Structure and Diet of Benthic Macrofauna in Invasive *Spartina Alterniflora* Wetlands Following Restoration With Native Mangroves. *Wetlands* 34, 673–683. doi: 10.1007/s13157-014-0533-2

Feng, J. X., Huang, Q., Chen, H., Guo, J. M., and Lin, G. H. (2018). Restoration of Native Mangrove Wetlands can Reverse Diet Shifts of Benthic Macrofauna Caused by Invasive Cordgrass. *J. Appl. Ecol.* 55 (2), 905–916. doi: 10.1111/1365-2664.12987

Garcia, A. F. S., Santos, M. L., Garcia, A. M., and Vieira, J. P. (2018). Changes in Food Web Structure of Fish Assemblages Along a River-to-Ocean Transect of a Coastal Subtropical System. *Mar. Freshwat. Res.* 70, 402–416. doi: 10.1071/MF18212

Hanson, C. E., Hyndes, G. A., and Wang, S. F. (2010). Differentiation of Benthic Marine Primary Producers Using Stable Isotopes and Fatty Acids: Implications to Food Web Studies. *Aquat. Bot.* 93 (2), 114–122. doi: 10.1016/j.aquabot.2010.04.004

Heck, K. L.Jr., Carruthers, T. J. B., Duarte, C. M., Hughes, A. R., Kendrick, G., Orth, R. J., et al. (2008). Trophic Transfers From Seagrass Meadows Subsidize Diverse Marine and Terrestrial Consumers. *Ecosystems* 11, 1198–1210. doi: 10.1007/s10021-008-9155-y

Hemminga, M. A., and Mateo, M. A. (1996). Stable Carbon Isotopes in Seagrasses: Variability in Ratios and Use in Ecological Studies. *Mar. Ecol. Progr. Ser.* 140, 285–298. doi: 10.3354/meps140285

Hoy, S. R., Vucetich, J. A., Liu, R. S., Deangelis, D. L., Peterson, R. O., Vucetich, L. M., et al. (2019). Negative Frequency-Dependent Foraging Behaviour in a Generalist Herbivore (*Alces Alces*) and its Stabilizing Influence on Food Web Dynamics. *J. Anim. Ecol.* 88 (9), 1291–1304. doi: 10.1111/1365-2656.13031

Islam, M. S., Yamashita, Y., and Tanaka, M. (2011). A Review on the Early Life History and Ecology of Japanese Sea Bass and Implication for Recruitment. *Environ. Biol. Fish.* 91, 389–405. doi: 10.1007/s10641-011-9798-y

Jackson, A. L., Parnell, A. C., Inger, R., and Bearhop, S. (2011). Comparing Isotopic Niche Widths Among and Within Communities: SIBER–Stable Isotope Bayesian Ellipses in R. *J. Anim. Ecol.* 80, 595–602. doi: 10.1111/j.1365-2656.2011.01806.x

Janousek, C. N., Thorne, K. M., and Takekawa, J. Y. (2019). Vertical Zonation and Niche Breadth of Tidal Marsh Plants Along the Northeast Pacific Coast. *Estuar. Coast.* 42, 85–98. doi: 10.1007/s12237-018-0420-9

Jones, A. G., Dubois, S. F., Desroy, N., and Fournier, J. (2021). Intertidal Ecosystem Engineer Species Promote Benthic-Pelagic Coupling and Diversify Trophic Pathways. *Mar. Ecol. Progr. Ser.* 660, 119–139. doi: 10.3354/meps13600

Kiljunen, M., Peltonen, H., Lehtiniemi, M., Uusitalo, L., Sinisalo, T., Norkko, J., et al. (2020). Benthic-Pelagic Coupling and Trophic Relationships in Northern Baltic Sea Food Webs. *Limnol. Oceanogr.* 65 (8), 1706–1722. doi: 10.1002/lno.11413

Kim, C., Kang, H. Y., Lee, Y. J., Yun, S. G., and Kang, C. K. (2020). Isotopic Variation of Macroinvertebrates and Their Sources of Organic Matter Along an Estuarine Gradient. *Estuar. Coast.* 43, 496–511. doi: 10.1007/s12237-019-00543-z

Kopp, D., Lefebvre, S., Cachera, M., Villanueva, M. C., and Ernande, B. (2015). Reorganization of a Marine Trophic Network Along an Inshore–Offshore Gradient Due to Stronger Pelagic–Benthic Coupling in Coastal Areas. *Progr. Oceanogr.* 130, 157–171. doi: 10.1016/j.pocean.2014.11.001

Kortsch, S., Primicerio, R., Aschan, M., Lind, S., Dolgov, A. V., and Planque, B. (2019). Food-Web Structure Varies Along Environmental Gradients in a High-Latitude Marine Ecosystem. *Ecography* 42, 295–308. doi: 10.1111/ecog.03443

Kortsch, S., Primicerio, R., Fossheim, M., Dolgov, A. V., and Aschan, M. (2015). Climate Change Alters the Structure of Arctic Marine Food Webs Due to Poleward Shifts of Boreal Generalists. *Proc. R. Soc B.* 282, 20151546. doi: 10.1098/rspb.2015.1546

Kundu, G. K., Kim, C., Kim, D., Bibi, R., Kim, H., and Kang, C. K. (2021). Phytoplankton Fuel Fish Food Webs in a Low-Turbidity Temperate Coastal Embayment: A Stable Isotope Approach. *Front. Mar. Sci.* 8, 751551. doi: 10.3389/fmars.2021.751551

Layman, C., Arrington, D., Montaña, C., and Post, D. (2007). Can Stable Isotope Ratios Provide for Community-Wide Measures of Trophic Structure? *Ecology* 88 (1), 42–48. doi: 10.1890/0012-9658(2007)88[42:CSIRPF]2.0.CO;2

Li, X. X., Yang, W., Li, S. Z., Sun, T., Bai, J. H., Pei, J., et al. (2020). Asymmetric Responses of Spatial Variation of Different Communities to a Salinity Gradient in Coastal Wetlands. *Mar. Environ. Res.* 158, 105008. doi: 10.1016/j.marenvres.2020.105008

Li, X. X., Yang, W., Sun, T., and Gaedke, U. (2021). Quantitative Food Web Structure and Ecosystem Functions in a Warm-Temperate Seagrass Bed. *Mar. Biol.* 168, 74. doi: 10.1007/s00227-021-03878-z

Li, X. X., Yang, W., Sun, T., and Su, L. Y. (2019). Framework of Multidimensional Macrobenthos Biodiversity to Evaluate Ecological Restoration in Wetlands. *Environ. Res. Lett.* 14, 054003. doi: 10.1088/1748-9326/ab142c

Lohrer, A. M., Thrush, S. F., Hewitt, J. E., and Kraan, C. (2015). The Up-Scaling of Ecosystem Functions in a Heterogeneous World. *Sci. Rep.* 5, 10349. doi: 10.1038/srep10349

Mao, Z. G., Gu, X. H., Zeng, Q. F., and Chen, H. H. (2016). Carbon Sources and Trophic Structure in a Macrophyte-Dominated Polyculture Pond Assessed by Stable-Isotope Analysis. *Freshwat. Biol.* 61, 1861–1873. doi: 10.1111/fwb.12821

Mao, D. H., Liu, M. Y., Wang, Z. M., Li, L., Man, W. D., Jia, M. M., et al. (2019). Rapid Invasion of *Spartina Alterniflora* in the Coastal Zone of Mainland China: Spatiotemporal Patterns and Human Prevention. *Sens. (Basel).* 19 (10), 2308. doi: 10.3390/s19102308

Marczak, L. B., Ho, C., Więski, K., Vu, H., Denno, R. F., and Pennings, S. C. (2011). Latitudinal Variation in Top-Down and Bottom-Up Control of a Salt Marsh Food Web. *Ecology* 92, 276–281. doi: 10.1890/10-0760.1

Masese, F. O., Abrantes, K. G., Gettel, G. M., Irvine, K., Bouillon, S., and McClain, M. E. (2018). Trophic Structure of an African Savanna River and Organic Matter Inputs by Large Terrestrial Herbivores: A Stable Isotope Approach. *Freshwat. Biol.* 63, 1365–1380. doi: 10.1111/fwb.13163

Mendonça, V., Madeira, C., Dias, M., Vermandele, F., Archambault, P., Dissanayake, A., et al. (2018). What's in a Tide Pool? Just as Much Food Web Network Complexity as in Large Open Ecosystems. *PloS One* 13 (7), e0200066. doi: 10.1371/journal.pone.0200066

Meng, W. Q., Feagin, R. A., Innocenti, R. A., Hu, B. B., He, M. X., and Li, H. Y. (2020). Invasion and Ecological Effects of Exotic Smooth Cordgrass *Spartina Alterniflora* in China. *Ecol. Eng.* 143, 105670. doi: 10.1016/j.ecoleng.2019.105670

Mittermayr, A., Fox, S. E., and Sommer, U. (2014). Temporal Variation in Stable Isotope Composition (δ^{13}c, δ^{15}n and δ^{34}s) of a Temperate *Zostera Marina* Food Web. *Mar. Ecol. Progr. Ser.* 505, 95–105. doi: 10.3354/meps10797

Mor, J. R., Ruhí, A., Tornés, E., Valcárcel, H., Muoz, I., and Sabater, S. (2018). Dam Regulation and Riverine Food-Web Structure in a Mediterranean River. *Sci. Tot. Environ.* 625, 301–310. doi: 10.1016/j.scitotenv.2017.12.296

Nordström, M. C., and Bonsdorff, E. (2017). Organic Enrichment Simplifies Marine Benthic Food Web Structure. *Limnol. Oceanogr.* 62, 2179–2188. doi: 10.1002/lno.10558

Nordström, M. C., Demopoulos, A. W. J., Whitcraft, C. R., Rismondo, A., McMillan, P., Gonzalez, J. P., et al. (2015). Food Web Heterogeneity and Succession in Created Saltmarshes. *J. Appl. Ecol.* 52, 1343–1354. doi: 10.1111/1365-2664.12473

O'Gorman, E., Zhao, L., Pichler, D., Adams, G., Friberg, N., Rall, B. C., et al. (2017). Unexpected Changes in Community Size Structure in a Natural Warming Experiment. *Nat. Clim. Change* 7, 659–663. doi: 10.1038/nclimate3368

Park, H. J., Kang, H. Y., Park, T. H., and Kang, C. K. (2017). Comparative Trophic Structures of Macrobenthic Food Web in Two Macrotidal Wetlands With and Without a Dike on the Temperate Coast of Korea as Revealed by Stable Isotopes. *Mar. Environ. Res.* 131, 134–145. doi: 10.1016/j.marenvres.2017.09.018

Park, H. J., Kwak, J. H., and Kang, C. K. (2015). Trophic Consistency of Benthic Invertebrates Among Diversified Vegetational Habitats in a Temperate Coastal Wetland of Korea as Determined by Stable Isotopes. *Estuar. Coast.* 38, 599–611. doi: 10.1007/s12237-014-9834-1

Parnell, A. C., Inger, R., Bearhop, S., and Jackson, A. L. (2010). Source Partitioning Using Stable Isotopes: Coping With Too Much Variation. *PloS One* 5, e9672. doi: 10.1371/journal.pone.0009672

Pennings, S. C., Grant, M. B., and Bertness, M. D. (2005). Plant Zonation in Low-Latitude Salt Marshes: Disentangling the Roles of Flooding, Salinity and Competition. *J. Ecol.* 93, 159–167. doi: 10.1111/j.1365-2745.2004.00959.x

Peterson, B. J., and Fry, B. (1987). Stable Isotopes in Ecosystem Studies. *Annu. Rev. Ecol. Syst.* 18, 293–320. doi: 10.1146/annurev.es.18.110187.001453

Post, D. M. (2002). Using Stable Isotopes to Estimate Trophic Position: Models, Methods, and Assumptions. *Ecology* 83, 703–718. doi: 10.1890/0012-9658(2002)083[0703:USITET]2.0.CO;2

Qi, M., Zhao, F., Sun, T., and Voinov, A. (2021). Disentangling the Relative Influence of Regeneration Processes on Marsh Plant Assembly With a Stage-Structured Plant Assembly Model. *Ecol. Model.* 455, 109646. doi: 10.1016/j.ecolmodel.2021.109646

Robson, B. J., Lester, R. E., Baldwin, D. S., Bond, N. R., Drouart, R., Rolls, R. J., et al. (2017). Modelling Food-Web Mediated Effects of Hydrological Variability and Environmental Flows. *Water Res.* 124, 108–128. doi: 10.1016/j.watres.2017.07.031

Rogers, K., Kelleway, J. J., Saintilan, N. J., Megonigal, P., Adams, J. B., Holmquist, J. R., et al. (2019). Wetland Carbon Storage Controlled by Millennial-Scale Variation in Relative Sea-Level Rise. *Nature* 567, 91–95. doi: 10.1038/s41586-019-0951-7

Saporiti, F., Bearhop, S., Vales, D. G., Silva, L., Zenteno, L., Tavares, M., et al. (2015). Latitudinal Changes in the Structure of Marine Food Webs in the Southwestern Atlantic Ocean. *Mar. Ecol. Progr. Ser.* 538, 23–34. doi: 10.3354/meps11464

Schrama, M., van der Plas, F., Berg, M. P., and Olff, H. (2017). Decoupled Diversity Dynamics in Green and Brown Webs During Primary Succession in a Saltmarsh. *J. Anim. Ecol.* 86, 158–169. doi: 10.1111/1365-2656.12602

Sierszen, M. E., Peterson, G. S., Trebitz, A. S., Brazner, J. C., and West, C. W. (2006). Hydrology and Nutrient Effects on Food-Web Structure in Ten Lake Superior Coastal Wetlands. *Wetlands* 26 (4), 951–964. doi: 10.1672/0277-5212(2006)26[951:HANEOF]2.0.CO;2

Thrush, S. F., Halliday, J., Hewitt, J. E., and Lohrer, A. M. (2008). The Effects of Habitat Loss, Fragmentation, and Community Homogenization on Resilience in Estuaries. *Ecol. Appl.* 18, 12–21. doi: 10.1890/07-0436.1

Tylianakis, J. M., and Morris, R. J. (2017). Ecological Networks Across Environmental Gradients. *Annu. Rev. Ecol. Evol. Syst.* 48, 25–48. doi: 10.1146/annurev-ecolsys-110316-022821

van der Lee, G. H., Vonk, J. A., Verdonschot, R. C. M., Kraak, M. H. S., Verdonschot, P. F. M., and Huisman, J. (2021). Eutrophication Induces Shifts in the Trophic Position of Invertebrates in Aquatic Food Webs. *Ecology* 102 (3), e03275. doi: 10.1002/ecy.3275

vander Zanden, M. J., Casselman, J. M., and Rasmussen, J. B. (1999). Stable Isotope Evidence for the Food Web Consequences of Species Invasions in Lakes. *Nature* 401, 464–467. doi: 10.1038/46762

Vermeiren, P., Abrantes, K., and Sheaves, M. (2015). Generalist and Specialist Feeding Crabs Maintain Discrete Trophic Niches Within and Among Estuarine Locations. *Estuar. Coast.* 38, 2070–2082. doi: 10.1007/s12237-015-9959-x

Vinagre, C., and Costa, M. J. (2014). Estuarine-Coastal Gradient in Food Web Network Structure and Properties. *Mar. Ecol. Progr. Ser.* 503, 11–21. doi: 10.3354/meps10722

Voigt, E. P., and Hovel, K. A. (2019). Eelgrass Structural Complexity Mediates Mesograzer Herbivory on Epiphytic Algae. *Oecologia* 189, 199–209. doi: 10.1007/s00442-018-4312-2

Wails, C. N., Baker, K., Blackburn, R., Vallé, A. D., Heise, J., Herakovich, H., et al. (2021). Assessing Changes to Ecosystem Structure and Function Following Invasion by *Spartina Alterniflora* and *Phragmites Australis*: A Meta-Analysis. *Biol. Invas.* 23 (9), 1–15. doi: 10.1007/s10530-021-02540-5

Williams, R. J. (2010). Network3D Software. (Cambridge, UK: Microsoft Research).

Wittyngham, S. S. (2021). Salinity and Simulated Herbivory Influence *Spartina Alterniflora* Traits and Defense Strategy. *Estuar. Coast.* 44, 1183–1192. doi: 10.1007/s12237-020-00841-x

Wozniak, A. S., Roman, C. T., Wainright, S. C., McKinney, R. A., and James-Pirri, M.-J. (2006). Monitoring Food Web Changes in Tide-Restored Salt Marshes: A Carbon Stable Isotope Approach. *Estuar. Coast.* 29, 568–578. doi: 10.1007/BF02784283

Yan, Z. Z., Xu, Y., Zhang, Q. Q., Qu, J. G., and Li, X. Z. (2019). Decomposition of *Spartina Alterniflora* and Concomitant Metal Release Dynamics in a Tidal Environment. *Sci. Tot. Environ.* 663, 867–877. doi: 10.1016/j.scitotenv.2019.01.422

Ye, F., Guo, W., Shi, Z., Jia, G. D., and Wei, G. J. (2017). Seasonal Dynamics of Particulate Organic Matter and its Response to Flooding in the Pearl River Estuary, China, Revealed by Stable Isotope (δ^{13}c and δ^{15}n) Analyses. *J. Geophys. Res. Ocean.* 122, 6835–6856. doi: 10.1002/2017JC012931

Yoon, I., Williams, R. J., Levine, E., Yoon, S., Dunne, J. A., and Martinez, N. D. (2004). Webs on the Web (WoW): 3D Visualization of Ecological Networks on the WWW for Collaborative Research and Education. *Proc. SPIE - Int. Soc. Opt. Eng.* 5295. 124–132. doi: 10.1117/12.526956

Young, M. J., Feyrer, F., Stumpner, P. R., Larwood, V., Patton, O., and Brown, L. R. (2021). Hydrodynamics Drive Pelagic Communities and Food Web Structure in a Tidal Environment. *Internat. Rev. Hydrobiol.* 106, 69–85. doi: 10.1002/iroh.202002063

Zhang, Y. H., Ding, W. X., Luo, J. F., and Donnison, A. (2010). Changes in Soil Organic Carbon Dynamics in an Eastern Chinese Coastal Wetland Following Invasion by a C4 Plant *Spartina Alterniflora*. *Soil Biol. Biochem.* 42 (10), 1712–1720. doi: 10.1016/j.soilbio.2010.06.006

Zhang, X. H., Zhang, Z. S., Li, Z., Li, M., Wu, H. T., and Jiang, M. (2021). Impacts of *Spartina Alterniflora* Invasion on Soil Carbon Contents and Stability in the Yellow River Delta, China. *Sci. Tot. Environ.* 775, 145188. doi: 10.1016/j.scitotenv.2021.145188

Conflict of Interest: The authors declare that the research was conducted in the absence of any commercial or financial relationships that could be construed as a potential conflict of interest.